RSC Medicinal Chemistry

ROYAL SOCIETY OF CHEMISTRY

RESEARCH ARTICLE

View Article Online
View Journal | View Issue

Cite this: *RSC Med. Chem.*, 2024, **15**, 2514

Design, synthesis, and structure–activity relationship studies of 6,7-dihydro-5*H*-pyrrolo[1,2-*b*][1,2,4]triazole derivatives as necroptosis inhibitors†

Zechen Jin,‡[ac] Yang Dai,‡[bc] Yinchun Ji,[b] Xia Peng,[b] Wenhu Duan,[acd] Jing Ai*[bc] and Hefeng Zhang *[a]

Received 16th April 2024,
Accepted 17th May 2024

DOI: 10.1039/d4md00265b

rsc.li/medchem

The development of necroptosis inhibitors has emerged as a promising strategy to effectively mitigate necroptosis-related inflammatory diseases, neurodegenerative diseases, and cancers. In this paper, we reported a series of 6,7-dihydro-5*H*-pyrrolo[1,2-*b*][1,2,4]triazole derivatives as potent necroptosis inhibitors. The representative compound **26** displayed potent anti-necroptotic activity in both human and mouse cellular assays and exhibited potent inhibitory activity against receptor-interacting protein kinase 1 (RIPK1). *In vivo* pharmacokinetic studies were performed to determine the oral exposure of compound **26**. Finally, molecular docking elucidated that compound **26** could effectively bind to the allosteric pocket of RIPK1 and serve as a type III inhibitor. Taken together, our findings highlighted that compound **26** represented a promising lead compound for future necroptosis inhibitor development.

Introduction

Necroptosis is an important form of programmed cell death (PCD). Although necroptosis shares certain characteristics with necrosis, it is precisely regulated by the receptor-interacting protein kinase (RIPK) family.[1] Generally, necroptosis is activated when apoptosis pathways are compromised. In the classic tumor necrosis factor receptor-α (TNF-α)-mediated necroptosis signaling pathway, RIPK1 is initially ubiquitinated and plays a central role in complex I.[2] When RIPK1 is deubiquitinated and complex I is disassociated, RIPK1 translocates to complex IIa/IIb to initiate PCD.[3,4] With the deficiency of caspase-8 in the cytoplasm, RIPK1, RIPK3, and mixed lineage kinase domain-like protein (MLKL) join together to form necrosomes, where RIPK1 triggers cascade phosphorylation and eventually initiates necroptosis (Fig. 1).[4] Although necroptosis is essential for some physiological processes such as nerve development, abnormal necroptosis could lead to various diseases.[5] Necroptosis upregulation has been implicated in autoimmune disorders such as systemic lupus erythematosus, neurodegenerative diseases including Alzheimer's disease and stroke-induced brain injury.[6–8] Necroptosis also promotes several cancers such as glioblastoma, lung cancer, pancreatic ductal adenocarcinoma, and ovarian carcinoma.[9–12] The development of necroptosis inhibitors may offer promising therapeutic strategies for the treatment of these diseases.

The development of RIPK1-targeted necroptosis inhibitors has aroused increased attention in recent years. Basing on different binding modes, current RIPK1 inhibitors are categorized into three classes: type I, II, and III (Fig. 2). Type I RIPK1 inhibitors are ATP-competitive inhibitors that interact with the DLG-in (Asp-Leu-Gly-in) conformation of RIPK1. Multitarget kinase inhibitors tozasertib (**1a**) and pazopanib (**1b**) are type I RIPK1 inhibitors with submicromolar level potency.[13,14] Type II RIPK1 inhibitors interact with DLG-out RIPK1 by occupying both the hinge region pocket and the allosteric pocket (Fig. 3A), thus exhibiting elevated bioactivity and selectivity. Compounds **2a** and **2b** are orally bioavailable type II RIPK1 inhibitors with favorable selectivity profiles.[15,16] A series of benzothiazole-based type II RIPK1 inhibitors were reported recently, and the representative compound **2c** demonstrated potent anti-

[a] *Small-Molecule Drug Research Center, Shanghai Institute of Materia Medica (SIMM), Chinese Academy of Sciences, 555 Zu Chong Zhi Road, Shanghai, 201203, China. E-mail: zhanghefeng1@simm.ac.cn*
[b] *Cancer Research Center, Shanghai Institute of Materia Medica (SIMM), Chinese Academy of Sciences, 555 Zu Chong Zhi Road, Shanghai, 201203, China. E-mail: jai@simm.ac.cn*
[c] *School of Pharmacy, University of Chinese Academy of Sciences, No. 19A Yuquan Road, Beijing, 100049, China*
[d] *Shandong Laboratory of Yantai Drug Discovery, Bohai Rim Advanced Research Institute for Drug Discovery, Yantai, Shandong, 264117, China*
† Electronic supplementary information (ESI) available. See DOI: https://doi.org/10.1039/d4md00265b
‡ These authors contributed equally to this work.

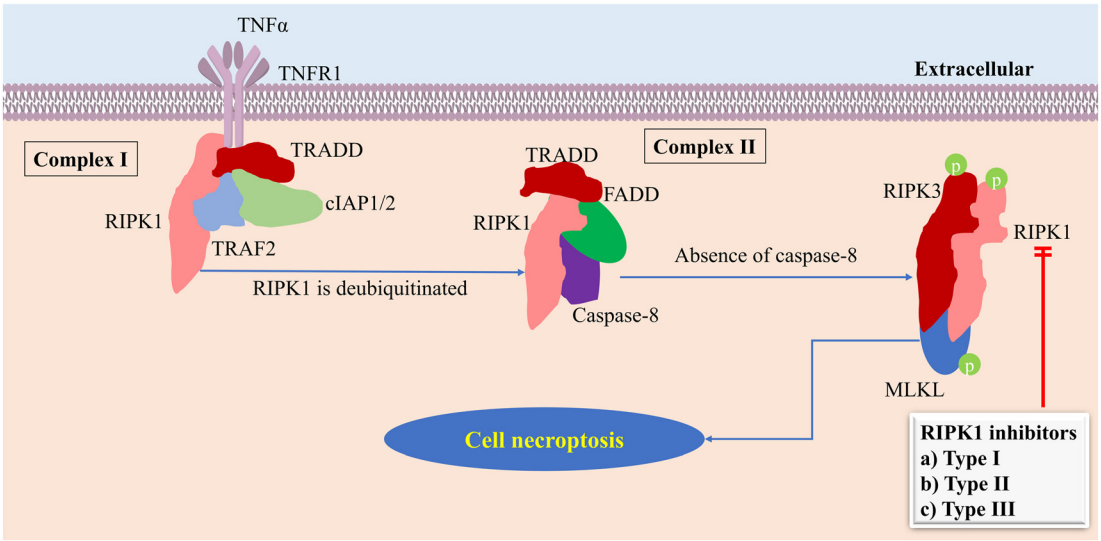

Fig. 1 Working mechanism of RIPK1 inhibitors in the RIPK1-necroptosis pathway.

necroptotic efficacy both *in vitro* and *in vivo*.[17–19] Type III inhibitors occupy the allosteric pocket of RIPK1 (Fig. 3B) and feature exceptional inhibitory potency and selectivity. Nec-1 (**3**) is the first type III selective RIPK1 inhibitor tool compound.[20] GSK2982772 (**4a**) has progressed into phase II clinical trials for treating several autoimmune diseases.[21,22] GSK3145095 (**4b**) has advanced into phase II clinical studies for cancer treatment (terminated).[23,24] Several analogs of **4a**, such as ZB-R-55 (**4c**), have been reported recently.[25–27] GSK′547 (**5**) stands out as a potent inhibitor against both human and murine RIPK1 (hRIPK1 and mRIPK1).[28] Compound **6** is another type III RIPK1 inhibitor which demonstrates strong anti-necroptotic activity against human-derived HT29 cells.[29]

In this paper, we reported a series of novel 6,7-dihydro-5*H*-pyrrolo[1,2-*b*][1,2,4]triazole-based type III RIPK1 inhibitors that displayed remarkable anti-necroptotic activity in both human and murine cells.

Results and discussion

Chemistry

The synthetic routes for compounds **7**–**20** are shown in Scheme 1. First, phenolic compounds **S1a–c** were treated with methyl 4-bromobutanoate to obtain carboxylic acid esters **S2a–c**. Treatment of esters **S2a–c** with methylmagnesium bromide afforded intermediates **S3a–c**, which underwent

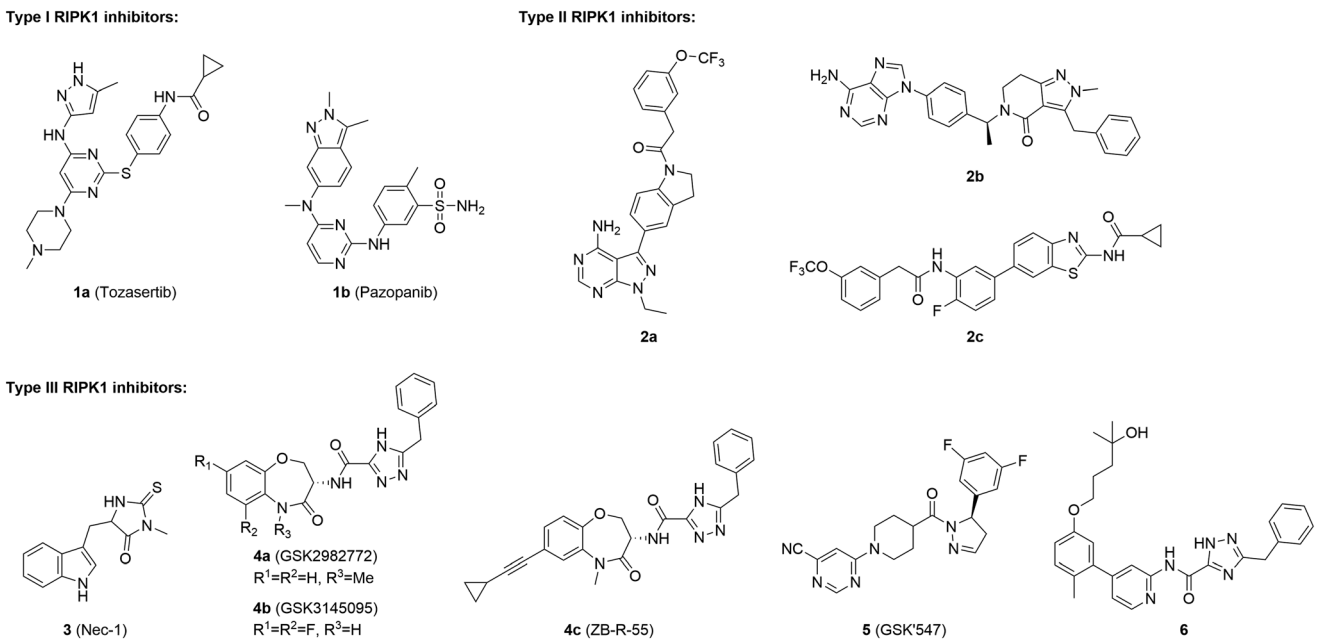

Fig. 2 Representative RIPK1 inhibitors.

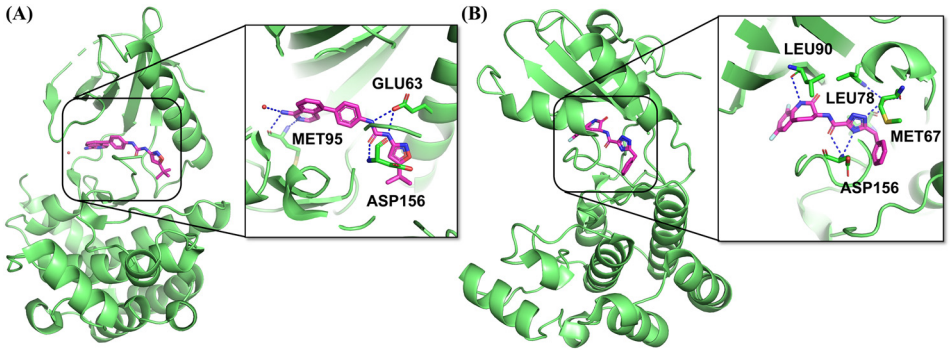

Fig. 3 Co-crystal structures and binding modes of the RIPK1 kinase domain complexed with (A) aminoisoquinoline-based type II inhibitor (PDB ID: 4NEU) or (B) type III inhibitor **4b** (PDB ID: 6RLN).

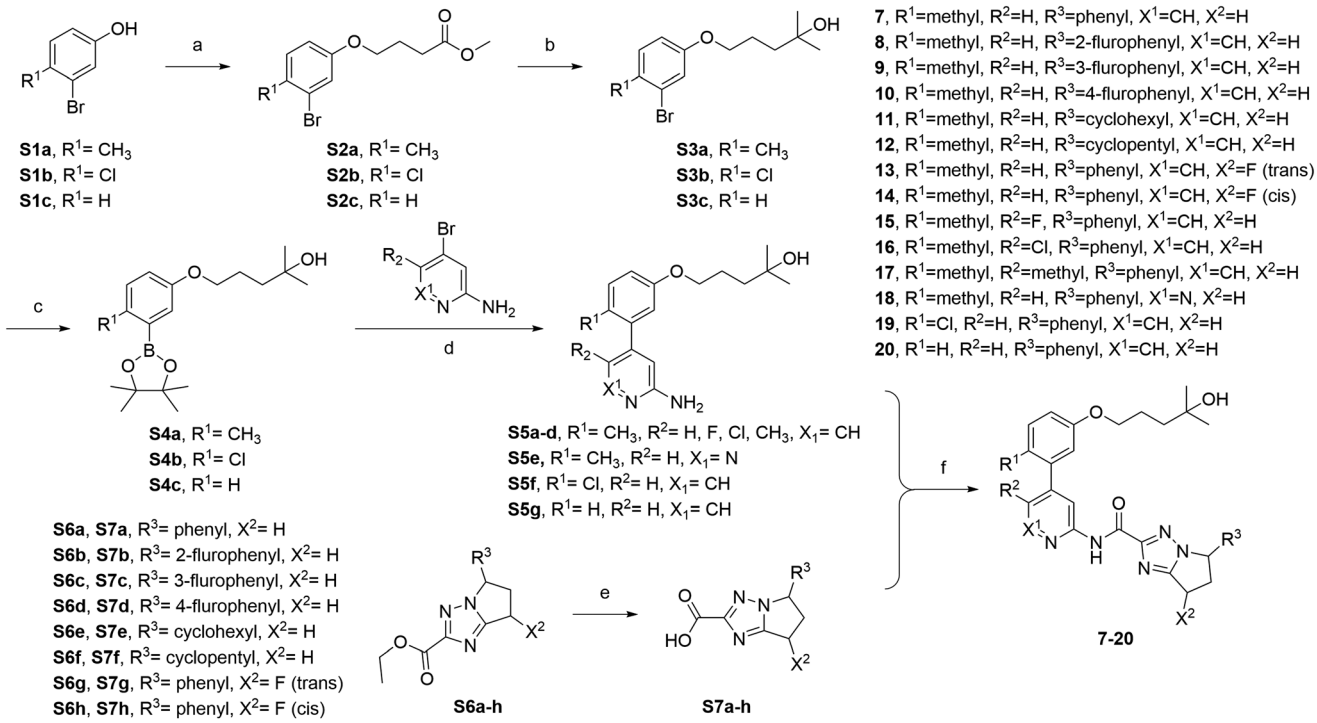

Scheme 1 Synthetic routes of the target compounds **7**–**20**. Reagents and conditions: (a) methyl 4-bromobutanoate, Cs_2CO_3, DMF, rt; (b) MeMgBr, THF, 0 °C; (c) bis(pinacolato)diboron, $Pd(dppf)Cl_2$, KOAc, 1,4-dioxane, 100 °C; (d) $Pd(dppf)Cl_2$, Na_2CO_3, 1,4-dioxane, H_2O, 100 °C; (e) 1 N LiOH, MeOH, rt; (f) *O*-(7-azabenzotriazol-1-yl)-*N*,*N*,*N*′,*N*′-tetramethyluronium hexafluorophosphate (HATU), *N*,*N*-diisopropylethylamine (DIPEA), DMF, rt.

Miyaura borylation and Suzuki coupling reactions to yield amines **S5a–g**. Finally, amines **S5a–g** were condensed with corresponding acids **S7a–h** to afford the target compounds **7–20**.

Compounds **21–28** were obtained *via* similar routes (Scheme 2). Phenol ethers **S8a–e** were obtained through nucleophilic substitution reactions. Then intermediates **S8a–e** underwent Suzuki coupling reactions with (2-aminopyridin-4-yl)boronic acid to give amines **S9a–e**. Finally, amines **S9a–e** were condensed with corresponding acids **S7a**, **S11a** or **S11b** to afford the target compounds **21–28**.

Design rationale and structure–activity relationship (SAR) studies

Compound **6** with good human cellular activity (HT29 IC_{50} < 100 nM in the literature) was selected at the starting point of our research.[29] The anti-TNF-α-induced necroptosis activity of compounds was evaluated using both human I2.1 cells and murine Hepa1-6 cells. Despite compound **6** demonstrating potent anti-necroptotic activity against I2.1 cells (90.0% recovery at 10 nM), it exhibited no recovery activity against Hepa1-6 cells (0% recovery at 1 μM). The species selectivity of compound **6** impedes its further biological evaluations in rodents, which should be addressed. It is noteworthy that GSK2982772, another RIPK1 inhibitor which features the 3-benzyl-4*H*-1,2,4-triazole moiety as the allosteric fragment, also exhibited species selectivity between hRIPK1 and mRIPK1 (hRIPK1 IC_{50} = 16 nM, mRIPK1 IC_{50} = 2.5 μM).[21] It was reported that such species difference might be attributed to the diminished flexibility of residues near

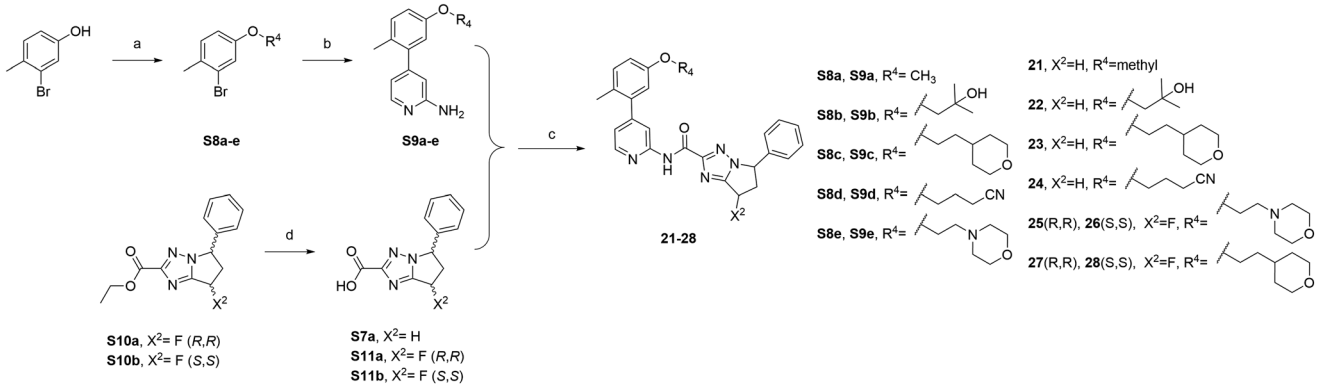

Scheme 2 Synthetic route of the target compounds **21–28**. Reagents and conditions: (a) corresponding bromides, Cs_2CO_3, DMF, rt; (b) (2-aminopyridin-4-yl)boronic acid, Pd(dppf)Cl_2, Na_2CO_3, 1,4-dioxane, H_2O, 100 °C; (c) HATU, DIPEA, DMF, rt; (d) 1 N LiOH, MeOH, rt.

the allosteric regions in mRIPK1.[26,28] This evidence shows us that the allosteric fragment of compound **6** requires further optimization to develop novel necroptosis inhibitors that are active for both human and murine cells.

Fig. 4 demonstrates our design rationale. Our attention was drawn to the hRIPK/mRIPK inhibitor GSK′547. The 5-phenyl-4,5-dihydro-1*H*-pyrazol-1-yl allosteric moiety of GSK′547 should be critical for its mRIPK1 inhibitory activity.[28] We adopted a cyclization design strategy and incorporated the allosteric structural feature of GSK′547 into compound **6**. As a result, the 6,7-dihydro-5*H*-pyrrolo[1,2-*b*][1,2,4]triazole derivative **7** was designed. Encouragingly, compound **7** showed a marked increase in anti-necroptotic activity for murine Hepa1-6 cells (86.6% recovery at 1 μM) while retaining potent anti-necroptotic efficacy for human I2.1 cells. Following this breakthrough, we conducted systematic SAR studies for compound **7**. Those compounds achieving over 75% recovery rate in I2.1 cells at 10 nM were further tested to determine their anti-necroptotic activities in Hepa1-6 cells.

Initially, we explored the terminal phenyl ring at the R^3-position and synthesized compounds **8–12** (Table 1). Introduction of a fluorine substituent at the ortho (compound **8**), meta (compound **9**), or para (compound **10**) position of the phenyl led to a slight decrease in activity. This result suggested

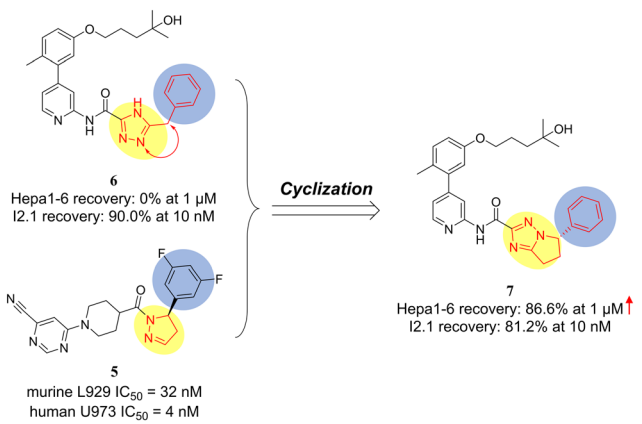

Fig. 4 Design rationale of compound **7**.

that additional substituents on the phenyl ring were unfavorable. Replacing the phenyl ring with cycloalkyls (compounds **11** and **12**) maintained the activity, indicating that the R^3 group interacts with the RIPK1 protein primarily through hydrophobic interactions, rather than π–π stacking. Considering both activity and molecular weight, unsubstituted phenyl was selected as the optimal substitution pattern for the R^3 group.

Next, we introduced a fluorine substituent at the 7′-position of the 6,7-dihydro-5*H*-pyrrolo[1,2-*b*][1,2,4]triazole moiety and afforded *cis*–*trans*-isomers **13** and **14** (Table 1). Both compounds **13** and **14** showed enhanced activity in Hepa1-6 cells, suggesting that 7′-fluoro might contribute to additional van der Waals interactions with mRIPK1. The *cis*-isomer **13** exhibited over 100-fold improved potency in Hepa1-6 cells compared to compound **7**. Consequently, the *cis*-substituted fluorine at the 7′-position was chosen as the preferred substitution pattern for this segment.

We next explored the SARs of the pyridine–phenyl moiety (compounds **15–20**, Table 1). Introduction of a halogen atom (**15** and **16**) or methyl group (**17**) at the R^2-position resulted in a slight loss in activity. This indicated that the R^2-position might be close to the pocket surface and could not accommodate additional substituents. Replacing the pyridine ring with pyridazine led to decreased potency (**18**). At the R^1-position, replacing the methyl group of compound **7** with a chlorine substituent (**19**) or removing the methyl group (**20**) diminished the activity in Hepa1-6 cells. The R^1-methyl group was presumed to restrain the appropriate dihedral angle of the pyridine–phenyl moiety.

We also investigated the SAR of the R^4 group (Table 2). Replacing the R^4 group of compound **7** with methyl (**21**) or cyanopropyl (**24**) resulted in decreased potency, which might be due to the reduced solubility of these compounds. Compounds **22** and **23** with hydrophilic groups as R^4 substituents exhibited elevated potency in both I2.1 and Hepa1-6 cells. Given the potential metabolic risk of the hydroxyl group, the 2-(tetrahydro-2*H*-pyran-4-yl)ethyl group of compound **23** was identified as the optimal substituent for the R^4 group.

Ultimately, we combined the advantageous substitution patterns of compounds **7**, **14**, and **23** and performed

Table 1 The anti-necroptotic activities of compounds **6–20**[a]

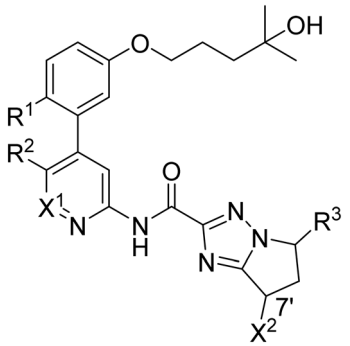

Compd	R^1	R^2	R^3	X^1	X^2	I2.1 recovery (%) at 10 nM	Hepa1-6 recovery (%) 1 μM	100 nM	10 nM
6	—	—	—	—	—	90.0 ± 14.1	<0	N.D.[b]	N.D.
7	CH_3	H		CH	H	81.2 ± 17.3	86.6 ± 4.3	26.1 ± 3.5	5.5 ± 0.1
8	CH_3	H		CH	H	62.7 ± 5.1	N.D.		
9	CH_3	H		CH	H	58.1 ± 3.4	N.D.		
10	CH_3	H		CH	H	60.1 ± 1.4	N.D.		
11	CH_3	H		CH	H	61.2 ± 1.5	N.D.		
12	CH_3	H		CH	H	73.2 ± 19.4	N.D.		
13	CH_3	H		CH	F(*trans*)	98.9 ± 1.6	104.2 ± 0.6	41.3 ± 1.3	6.3 ± 1.3
14	CH_3	H		CH	F(*cis*)	80.6 ± 0.6	110.0 ± 4.5	107.6 ± 5.3	100.5 ± 3.3
15	CH_3	F		CH	H	58.1 ± 16.5	N.D.		
16	CH_3	Cl		CH	H	56.2 ± 9.1	N.D.		
17	CH_3	CH_3		CH	H	72.7 ± 5.2	N.D.		
18	CH_3	H		N	H	53.6 ± 6.2	N.D.		
19	Cl	H		CH	H	80.6 ± 0.6	2.9 ± 0.1	N.D.	N.D.
20	H	H		CH	H	86.1 ± 19.7	2.2 ± 0.7	N.D.	N.D.

[a] These data are the mean ± SD values of at least two assays. [b] N.D. refers to not determined.

appropriate derivatizations to synthesize compounds **25–28** with absolute configurations. Additionally, we tested their RIPK1 inhibitory activities at a concentration of 1 μM (Table 3). The results indicated that compounds **25** and **27** with "*R*,*R*" chiral centers had no RIPK1 inhibitory effect. This consequence highlighted the critical impact of the absolute configuration on this series of compounds: the 5′-(*R*) configuration should have impeded the extension of the 5′-phenyl into the hydrophobic pocket of RIPK1. In contrast, the "*S*,*S*"-configured compounds **26** and **28** showed satisfactory RIPK1 inhibitory activity and cellular recovery efficacy. Compound **26** which features a morpholine fragment at the R^4-substituent exhibited superior activity in I2.1 cells. Therefore, compound **26** was selected for further studies.

Pharmacokinetic properties of compound 26

We evaluated the pharmacokinetic properties of compound **26** in SD rats ($N = 3$) at a dose of 3 mg kg^{-1} (p.o.). The plasma concentrations of compound **26** were monitored for 24 h. As

Table 2 The anti-necroptotic activities of compounds **21–24**[a]

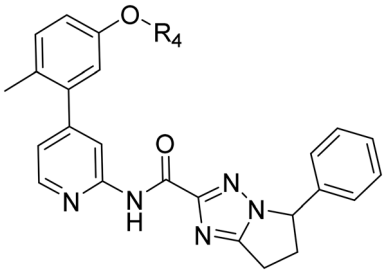

Compd	R^4	I2.1 recovery (%) at 10 nM	Hepa1-6 recovery (%) 1 μM	100 nM	10 nM
21	CH_3	73.7 ± 1.8	N.D.[b]		
22		98.2 ± 1.9	94.1 ± 0.5	10.9 ± 1.3	3.8 ± 1.3
23	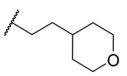	91.9 ± 8.2	96.6 ± 5.2	10.7 ± 2.5	3.7 ± 1.6
24	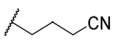	35.8 ± 5.8	N.D.		

[a] These data are the mean ± SD values of at least two assays. [b] N.D. refers to not determined.

Table 3 The anti-necroptotic and RIPK1 inhibition activities of compounds **25–28**[a]

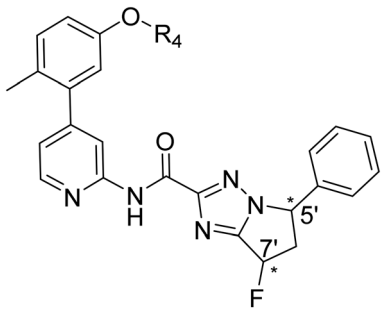

Compd	R^4	Stereo (5′,7′)	RIPK1 inhibition (%) at 1 μM	I2.1 recovery (%) at 10 nM	Hepa1-6 recovery (%) at 10 nM
25	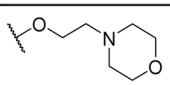	*R*,*R*	<0	N.D.[b]	N.D.
26	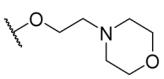	*S*,*S*	79.1 ± 5.2	97.9 ± 3.0	102.4 ± 0.2
27	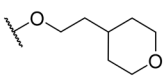	*R*,*R*	<0	N.D.	N.D.
28	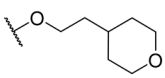	*S*,*S*	78.8 ± 1.7	70.5 ± 9.1	111.4 ± 2.1

[a] These data are the mean ± SD values of at least two assays. [b] N.D. refers to not determined.

Table 4 Pharmacokinetic parameters of **26** in rats after p.o. administration[a]

Compd (3 mg kg^{-1})	$T_{1/2}$ (h)	T_{max} (h)	C_{max} (ng mL^{-1})	AUC_{last} (h ng mL^{-1})
26	1.91	0.67	8.90	15.2

[a] $N = 3$, data are shown as mean values.

shown in Table 4, compound **26** reached a low peak plasma concentration (C_{max}) of 8.90 ng mL^{-1} at 0.67 h. The elimination half-life ($T_{1/2}$) of compound **26** was determined to be 1.91 h, suggesting a moderate duration of presence in the systemic circulation. Additionally, the area under the curve (AUC), a critical measure of the drug's overall presence in the plasma over time, was calculated to be 15.2 h ng mL^{-1}.

Molecular docking

Molecular docking was conducted to elucidate the binding mode of compound **26**. Fig. 5 illustrates that compound **26** effectively occupied the allosteric hydrophobic pocket of RIPK1 and formed two critical hydrogen bonds with ASP156. The 6,7-dihydro-5*H*-pyrrolo[1,2-*b*][1,2,4]triazole ring and the 7′-fluoro substituent interacted with RIPK1 primarily through hydrophobic interactions. Additionally, the morpholine fragment formed two salt bridge interactions with ASN99 and GLU142. The pyridine–phenyl moiety adopted a cross conformation and acted as a linker connecting the allosteric segment with the solvent moiety. In summary, compound **26** was a potential type III RIPK1 inhibitor.

Conclusion

The development of necroptosis inhibitors has attracted widespread attention for their potential applications in autoimmune diseases, neurodegenerative diseases, and cancers. In this study, we started with the human-cell specific necroptosis inhibitor compound **6** and employed a cyclization design strategy to synthesize a series of 6,7-dihydro-5*H*-pyrrolo[1,2-*b*][1,2,4]triazole derivatives as potent necroptosis inhibitors. These compounds exhibited potent anti-necroptotic activity against both human and murine cells. Systematic SAR studies led to the optimum compound **26**. Compound **26** demonstrated robust anti-necroptotic activity in both human I2.1 and murine Hepa1-6 cells and significantly inhibited RIPK1 enzymatic activity. *In vivo* pharmacokinetic evaluation demonstrated that compound **26** displayed relatively low oral exposure. Molecular docking revealed that compound **26** served as a potential type III RIPK1 inhibitor and effectively bound to the allosteric pocket of RIPK1. In summary, compound **26** represents a promising lead compound for future development of necroptosis inhibitors.

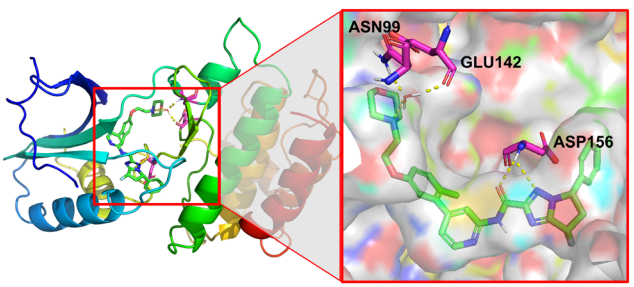

Fig. 5 Proposed binding mode of compound **26** with RIPK1 (PDB 6NYH). Interactions of compound **26** (green) and amino acid residues (magenta) are shown.

Experimental section

Chemistry

Unless specifically stated, all reagents and solvents were obtained from commercial sources and used without further purification. Reactions were generally carried out under an argon atmosphere unless otherwise stated. NMR spectra were obtained on Varian Mercury 400 or Bruker AVANCE NMR 400, 500, 600 spectrometers. ^{1}H and ^{13}C NMR spectra were obtained at 400/600 MHz and 126/151 MHz, respectively. The chemical shifts were reported in ppm relative to trimethylsilane or deuterated solvents (chloroform-*d*, DMSO-d_6, methanol-d_4, acetone-d_6) as internal standards. The observed splitting patterns were designated as "s" for singlet, "d" for doublet, "t" for triplet, "q" for quartet, and "m" for multiplet, respectively. Mass spectrometric analysis was performed using an Agilent 6110 Quadrupole LC/MS in ESI-MS mode. High-resolution mass spectrometry (HR-MS) was conducted on an Agilent G6520 Q-TOF spectrometer (ESI-MS mode). Purity assessment of all compounds (>95%) was performed using an Agilent Infinity 1260 high-performance liquid chromatography (HPLC) system.

Preparation procedure of compounds 7–28

Methyl 4-(3-bromo-4-methylphenoxy)butanoate (S2a). To a mixture of 3-bromo-4-methylphenol (1.0 g, 5.35 mmol) and cesium carbonate (5.2 g, 16.04 mmol) in *N*,*N*-dimethylformamide (DMF, 5 mL) was added methyl 4-bromobutanoate (675 μL, 5.35 mmol). The resulting mixture was stirred for 12 h. The reaction was quenched with water (20 mL) and the mixture was extracted with ethyl acetate (30 mL × 3). The organic layers were combined, washed with saturated brine (30 mL × 5), dried over anhydrous sodium sulfate and concentrated under reduced pressure to obtain intermediate **S2a** as a pale-yellow oil (1.53 g, 99%). ^{1}H NMR (400 MHz, chloroform-*d*) δ 7.12–7.06 (m, 2H), 6.76–6.72 (m, 1H), 3.96 (t, J = 6.0 Hz, 2H), 3.69 (s, 3H), 2.51 (t, J = 7.2 Hz, 2H), 2.31 (s, 3H), 2.13–2.04 (m, 2H). MS (ESI) m/z: 309.0 [M + Na]$^+$.

5-(3-Bromo-4-methylphenoxy)-2-methylpentan-2-ol (S3a). Methyl magnesium bromide (3 M in tetrahydrofuran, 5.29 mL, 15.88 mmol) was added dropwise to a solution of intermediate **S2a** (1.52 g, 5.29 mmol) at 0 °C under an argon atmosphere. The resulting mixture was then warmed to room temperature and stirred for 5 h. After completion, the reaction was quenched with saturated ammonium chloride solution (50 mL) at 0 °C, and the aqueous phase was extracted with ethyl acetate (30 mL × 3). The organic phases were combined, washed with brine, dried over anhydrous sodium sulfate and concentrated under reduced pressure. The resulting residue was purified by flash chromatography (0% to 20% ethyl acetate in petroleum ether) to afford intermediate **S3a** as a pale-yellow oil (1.26 g, 83%). ^{1}H NMR

(400 MHz, chloroform-*d*) δ 7.13–7.07 (m, 2H), 6.75 (dt, J = 8.4, 2.7 Hz, 1H), 3.93 (td, J = 6.5, 2.7 Hz, 2H), 2.31 (d, J = 2.8 Hz, 3H), 1.90–1.83 (m, 2H), 1.67–1.59 (m, 2H), 1.26 (d, J = 3.3 Hz, 7H). MS (ESI) m/z: 309.0 $[M + Na]^+$.

2-Methyl-5-(4-methyl-3-(4,4,5,5-tetramethyl-1,3,2-dioxaborolan-2-yl)phenoxy)pentan-2-ol (S4a). 5-(3-Bromo-4-methylphenoxy)-2-methylpentan-2-ol (**S3a**, 710 mg, 2.47 mmol), bis(pinacolato)diboron (753 mg, 2.97 mmol), [1,1′-bis(diphenylphosphino)ferrocene]dichloropalladium (217 mg, 0.297 mmol) and potassium acetate (728 mg, 7.42 mmol) were added to 1,4-dioxane (10 mL). The resulting mixture was degassed with argon three times and stirred at 100 °C for 10 h. The mixture was concentrated under reduced pressure, and the residue was purified by flash chromatography (0% to 20% ethyl acetate in petroleum ether) to afford intermediate **S4a** as a white solid (860 mg, 99%). ^{1}H NMR (400 MHz, DMSO-d_6) δ 7.10 (d, J = 2.9 Hz, 1H), 7.07 (d, J = 8.4 Hz, 1H), 6.90 (dd, J = 8.4, 2.9 Hz, 1H), 3.89 (t, J = 6.5 Hz, 2H), 2.37 (s, 3H), 1.77–1.66 (m, 2H), 1.51–1.44 (m, 2H), 1.29 (s, 12H), 1.09 (s, 6H). MS (ESI) m/z: 357.3 $[M + Na]^+$.

5-(3-(2-Aminopyridin-4-yl)-4-methylphenoxy)-2-methylpentan-2-ol (S5a). To a mixture of **S4a** (131 mg, 0.393 mmol), 4-bromopyridin-2-amine (45 mg, 0.262 mmol), and sodium carbonate (83 mg, 0.786 mmol) in 1,4-dioxane (4 mL) and water (1 mL) was added [1,1′-bis(diphenylphosphino)ferrocene]dichloropalladium (19 mg, 0.0262 mmol). The mixture was degassed with argon three times, and stirred at 100 °C for 3 h. After completion, the mixture was concentrated under vacuum. The residue was purified by flash chromatography (0% to 30% ethyl acetate in petroleum ether) to afford intermediate **S5a** as a brown solid (50 mg, 64%). ^{1}H NMR (400 MHz, chloroform-*d*) δ 8.09 (d, J = 5.3 Hz, 1H), 7.17 (d, J = 8.3 Hz, 1H), 6.88–6.82 (m, 1H), 6.76 (t, J = 2.1 Hz, 1H), 6.66–6.62 (m, 1H), 6.46 (s, 1H), 4.57 (s, 2H), 4.00 (t, J = 6.7 Hz, 2H), 2.21 (d, J = 1.5 Hz, 3H), 1.96–1.89 (m, 2H), 1.70–1.63 (m, 2H), 1.28 (s, 6H). MS (ESI) m/z: 301.2 $[M + H]^+$.

Ethyl 5-phenyl-6,7-dihydro-5*H*-pyrrolo[1,2-*b*][1,2,4]triazole-2-carboxylate (S6a). Intermediate **S6a** was synthesized according to the literature.[30] ^{1}H NMR (400 MHz, chloroform-*d*) δ 7.39–7.30 (m, 3H), 7.11–7.06 (m, 2H), 5.48 (dd, J = 8.4, 5.2 Hz, 1H), 4.52–4.38 (m, 2H), 3.29–3.18 (m, 1H), 3.18–3.09 (m, 1H), 3.09–2.99 (m, 1H), 2.72–2.62 (m, 1H), 1.40 (t, J = 7.1 Hz, 3H). MS (ESI) m/z: 258.1 $[M + H]^+$.

5-Phenyl-6,7-dihydro-5*H*-pyrrolo[1,2-*b*][1,2,4]triazole-2-carboxylic acid (S7a). To a solution of compound **S6a** (450 mg, 1.75 mmol) in methanol (10 mL) was added 1 M lithium hydroxide (aq, 3.27 mL, 3.27 mmol). The mixture was stirred for 3 h before completion. The solvent was removed under vacuum, and dissolved with water. Then 1 M hydrochloric acid was added dropwise to adjust the pH to 1–2 and a white precipitate formed. The precipitate was filtered, washed with water (5 mL) and dried under vacuum to afford intermediate **S7a** as a white solid (380 mg, 95%). ^{1}H NMR (400 MHz, DMSO-d_6) δ 13.12 (s, 1H), 7.44–7.33 (m, 3H), 7.27–7.21 (m, 2H), 5.57 (dd, J = 8.0, 6.0 Hz, 1H), 3.23–3.14 (m, 1H), 3.14–3.05 (m, 1H), 3.03–2.94 (m, 1H), 2.61–2.52 (m, 1H). MS (ESI) m/z: 228.2 $[M–H]^-$.

***N*-(4-(5-((4-Hydroxy-4-methylpentyl)oxy)-2-methylphenyl)pyridin-2-yl)-5-phenyl-6,7-dihydro-5*H*-pyrrolo[1,2-*b*][1,2,4]triazole-2-carboxamide (7).** To a solution of compound **S7a** (30 mg, 0.100 mmol), HATU (38 mg, 0.100 mmol) and DIPEA (43 μL, 0.250 mmol) in DMF (1 mL) was added intermediate **S5a** (19 mg, 0.0832 mmol). The resulting mixture was stirred at room temperature for 12 h. After completion, the reaction was quenched with water and the solution was extracted with ethyl acetate (30 mL × 3). The organic layers were combined, washed with saturated brine (20 mL × 5), dried over anhydrous sodium sulfate and concentrated under reduced pressure. The residue was purified by preparative thin layer chromatography to obtain the title compound as a white solid. (23 mg, 54%) ^{1}H NMR (400 MHz, acetone-d_6) δ 9.58 (s, 1H), 8.39 (d, J = 5.1 Hz, 1H), 8.33 (s, 1H), 7.44–7.29 (m, 5H), 7.23 (d, J = 8.4 Hz, 1H), 7.16 (dd, J = 5.1, 1.6 Hz, 1H), 6.92 (dd, J = 8.4, 2.7 Hz, 1H), 6.85 (d, J = 2.8 Hz, 1H), 5.67 (dd, J = 8.3, 5.9 Hz, 1H), 4.02 (t, J = 6.6 Hz, 2H), 3.45–3.33 (m, 1H), 3.25 (s, 1H), 3.23–3.17 (m, 1H), 3.16–3.07 (m, 1H), 2.76–2.70 (m, 1H), 2.23 (s, 3H), 1.93–1.83 (m, 2H), 1.64–1.56 (m, 2H), 1.19 (s, 6H). ^{13}C NMR (126 MHz, DMSO-d_6) δ 162.7, 160.6, 157.2, 156.9, 151.1, 150.7, 148.3, 139.5, 139.3, 131.8, 128.9, 128.4, 126.8, 126.1, 120.7, 114.9, 114.6, 113.7, 68.5, 68.3, 61.1, 35.4, 29.3, 24.0, 20.6, 19.0. HRMS: calcd for $C_{30}H_{34}N_5O_3$ $[M + H]^+$, 512.2662; found, 512.2657.

Intermediates **S6g**, **S6h**, **S10a** and **S10b** were synthesized according to the literature.[31,32]

(*R*,*R*)-Ethyl-7-fluoro-5-phenyl-6,7-dihydro-5*H*-pyrrolo[1,2-*b*][1,2,4]triazole-2-carboxylate (S10a), (*S*,*S*)-ethyl-7-fluoro-5-phenyl-6,7-dihydro-5*H*-pyrrolo[1,2-*b*][1,2,4]triazole-2-carboxylate (S10b) and *trans*-ethyl-7-fluoro-5-phenyl-6,7-dihydro-5*H*-pyrrolo[1,2-*b*][1,2,4]triazole-2-carboxylate (S6g). ^{1}H NMR (400 MHz, chloroform-*d*) δ 7.45–7.37 (m, 3H), 7.17–7.13 (m, 2H), 6.10 (ddd, J = 55.4, 6.4, 1.3 Hz, 1H), 5.75 (td, J = 6.7, 3.1 Hz, 1H), 4.59–4.41 (m, 2H), 3.50–3.35 (m, 1H), 3.14–2.95 (m, 1H), 1.44 (t, J = 7.1 Hz, 4H). MS (ESI) m/z: 276.3 $[M + H]^+$.

***cis*-Ethyl-7-fluoro-5-phenyl-6,7-dihydro-5*H*-pyrrolo[1,2-*b*][1,2,4]triazole-2-carboxylate (S6h).** ^{1}H NMR (400 MHz, chloroform-*d*) δ 7.42–7.34 (m, 3H), 7.23 (dd, J = 7.5, 2.0 Hz, 2H), 6.02 (ddd, J = 55.7, 7.1, 1.6 Hz, 1H), 5.50 (ddd, J = 8.8, 6.2, 2.7 Hz, 1H), 4.52–4.40 (m, 2H), 3.72–3.55 (m, 1H), 3.03–2.87 (m, 1H), 1.42 (t, J = 7.1 Hz, 3H). MS (ESI) m/z: 276.3 $[M + H]^+$.

Compounds **8–28** were synthesized *via* similar routes to compound **7**.

5-(2-Fluorophenyl)-*N*-(4-(5-((4-hydroxy-4-methylpentyl)oxy)-2-methylphenyl)pyridin-2-yl)-6,7-dihydro-5*H*-5λ^3-pyrrolo[1,5-*b*][1,2,4]triazole-2-carboxamide (8). Purified by preparative thin layer chromatography (dichloromethane : methanol = 20 : 1, V : V) as a white solid, yield 58%. ^{1}H NMR (400 MHz, methanol-d_4) δ 8.38 (d, J = 5.1 Hz, 1H), 8.27 (s, 1H), 7.48–7.39 (m, 1H), 7.28–7.16 (m, 5H), 6.92 (dd, J = 8.4, 2.7 Hz, 1H), 6.82 (d, J = 2.7 Hz, 1H), 5.86 (dd, J = 8.6, 5.8 Hz, 1H), 4.01 (t, J = 6.4 Hz, 2H), 3.42–3.36 (m, 1H), 3.28–3.11 (m, 2H), 2.82–2.72

(m, 1H), 2.24 (s, 3H), 1.93–1.81 (m, 2H), 1.67–1.62 (m, 2H), 1.23 (s, 6H). ^{13}C NMR (126 MHz, DMSO-d_6) δ 162.8, 160.7, 160.0 ($^{1}J_{C-F}$ = 247.0 Hz), 157.2, 157.0, 150.9 ($^{2}J_{C-F}$ = 58.0 Hz), 148.3, 139.5, 131.8, 130.7 ($^{3}J_{C-F}$ = 8.4 Hz), 128.9 ($^{4}J_{C-F}$ = 3.0 Hz), 126.1, 126.0 ($^{3}J_{C-F}$ = 12.5 Hz), 124.9, 120.7, 116.0, 115.9, 114.9, 114.6, 113.8, 68.5, 68.3, 56.1, 34.0, 29.3, 24.0, 20.6, 19.0. HRMS: calcd for $C_{30}H_{33}FN_5O_3$ $[M + H]^+$, 530.2567; found, 530.2563.

5-(3-Fluorophenyl)-*N*-(4-(5-((4-hydroxy-4-methylpentyl)oxy)-2-methylphenyl)pyridin-2-yl)-6,7-dihydro-5*H*-5λ^3-pyrrolo[1,5-*b*][1,2,4]triazole-2-carboxamide (9). Purified by preparative thin layer chromatography (dichloromethane : methanol = 20 : 1, V : V) as a white solid, yield 56%. ^{1}H NMR (400 MHz, methanol-d_4) δ 8.38 (d, J = 5.2 Hz, 1H), 8.28 (s, 1H), 7.51–7.41 (m, 1H), 7.23 (d, J = 8.4 Hz, 1H), 7.18 (d, J = 5.2 Hz, 1H), 7.17–7.06 (m, 3H), 6.92 (dd, J = 8.4, 2.8 Hz, 1H), 6.83 (d, J = 2.7 Hz, 1H), 5.69–5.62 (m, 1H), 4.01 (t, J = 6.4 Hz, 2H), 3.30–3.07 (m, 3H), 2.78–2.68 (m, 1H), 2.25 (s, 3H), 1.92–1.82 (m, 2H), 1.69–1.60 (m, 2H), 1.23 (s, 6H). ^{13}C NMR (126 MHz, DMSO-d_6) δ 162.9, 162.4 ($^{1}J_{C-F}$ = 244.0 Hz), 160.7, 157.1 ($^{2}J_{C-F}$ = 32.0 Hz), 151.1, 150.7, 148.3, 142.0 ($^{3}J_{C-F}$ = 7.1 Hz), 139.5, 131.8, 130.9 ($^{3}J_{C-F}$ = 8.0 Hz), 126.1, 123.0, 120.7, 115.3, 115.2, 114.9, 114.6, 113.8, 113.7 ($^{2}J_{C-F}$ = 21.0 Hz), 68.5, 68.3, 60.4, 35.2, 29.3, 24.0, 20.6, 19.0. HRMS: calcd for $C_{30}H_{33}FN_5O_3$ $[M + H]^+$, 530.2567; found, 530.2560.

5-(4-Fluorophenyl)-*N*-(4-(5-((4-hydroxy-4-methylpentyl)oxy)-2-methylphenyl)pyridin-2-yl)-6,7-dihydro-5*H*-5λ^3-pyrrolo[1,5-*b*][1,2,4]triazole-2-carboxamide (10). Purified by preparative thin layer chromatography (dichloromethane : methanol = 20 : 1, V : V) as a white solid, yield 55%. ^{1}H NMR (400 MHz, DMSO-d_6) δ 9.90 (s, 1H), 8.42 (d, J = 5.1 Hz, 1H), 8.10 (d, J = 1.3 Hz, 1H), 7.38 (dd, J = 8.7, 5.4 Hz, 2H), 7.30–7.19 (m, 4H), 6.93 (dd, J = 8.4, 2.7 Hz, 1H), 6.80 (d, J = 2.7 Hz, 1H), 5.67 (t, J = 7.2 Hz, 1H), 4.19 (s, 1H), 3.97 (t, J = 6.6 Hz, 2H), 3.26–3.01 (m, 4H), 2.19 (s, 3H), 1.80–1.70 (m, 2H), 1.52–1.43 (m, 2H), 1.10 (s, 6H). ^{13}C NMR (126 MHz, DMSO-d_6) δ 162.6, 162.0 ($^{1}J_{C-F}$ = 244.0 Hz), 160.6, 157.1 ($^{2}J_{C-F}$ = 31.0 Hz), 151.1, 150.7, 148.3, 139.5, 135.4, 131.8, 129.1 ($^{3}J_{C-F}$ = 8.1 Hz), 126.1, 120.7, 115.8, 115.6, 114.9, 114.6, 113.7, 68.5, 68.3, 60.4, 35.3, 29.3, 24.0, 20.6, 19.0. HRMS: calcd for $C_{30}H_{33}FN_5O_3$ $[M + H]^+$, 530.2567; found, 530.2562.

5-Cyclohexyl-*N*-(4-(5-((4-hydroxy-4-methylpentyl)oxy)-2-methylphenyl)pyridin-2-yl)-6,7-dihydro-5*H*-5λ^3-pyrrolo[1,5-*b*][1,2,4]triazole-2-carboxamide (11). Purified by preparative thin layer chromatography (dichloromethane : methanol = 20 : 1, V : V) as a white solid, yield 52%. ^{1}H NMR (400 MHz, methanol-d_4) δ 8.39 (d, J = 5.1 Hz, 1H), 8.30 (s, 1H), 7.23 (d, J = 8.4 Hz, 1H), 7.18 (dd, J = 5.2, 1.4 Hz, 1H), 6.91 (dd, J = 8.5, 2.7 Hz, 1H), 6.83 (d, J = 2.7 Hz, 1H), 4.43–4.34 (m, 1H), 4.00 (t, J = 6.4 Hz, 2H), 3.02–2.93 (m, 2H), 2.89–2.80 (m, 2H), 2.66–2.53 (m, 1H), 2.25 (s, 3H), 2.03–1.75 (m, 8H), 1.75–1.60 (m, 4H), 1.51–1.41 (m, 2H), 1.23 (s, 6H). ^{13}C NMR (126 MHz, DMSO-d_6) δ 162.2, 160.0, 157.3, 156.9, 151.1, 150.7, 148.3, 139.6, 131.8, 126.1, 120.6, 114.9, 114.6, 113.7, 68.5, 68.3, 62.3, 41.1, 29.3, 28.2, 27.7, 27.1, 25.7, 25.4, 24.0, 20.5, 19.0. HRMS: calcd for $C_{30}H_{40}N_5O_3$ $[M + H]^+$, 518.3131; found, 518.3124.

5-Cyclopentyl-*N*-(4-(5-((4-hydroxy-4-methylpentyl)oxy)-2-methylphenyl)pyridin-2-yl)-6,7-dihydro-5*H*-5λ^3-pyrrolo[1,5-*b*][1,2,4]triazole-2-carboxamide (12). Purified by preparative thin layer chromatography (dichloromethane : methanol = 20 : 1, V : V) as a white solid, yield 70%. ^{1}H NMR (400 MHz, acetone-d_6) δ 9.59 (s, 1H), 8.40 (d, J = 5.1 Hz, 1H), 8.35 (d, J = 1.4 Hz, 1H), 7.24 (d, J = 8.4 Hz, 1H), 7.16 (dd, J = 5.2, 1.6 Hz, 1H), 6.92 (dd, J = 8.4, 2.8 Hz, 1H), 6.86 (d, J = 2.7 Hz, 1H), 4.43 (td, J = 8.0, 4.8 Hz, 1H), 4.03 (t, J = 6.6 Hz, 2H), 3.30 (s, 1H), 3.00–2.91 (m, 3H), 2.58–2.47 (m, 1H), 2.36–2.26 (m, 1H), 2.24 (s, 3H), 2.03–1.96 (m, 1H), 1.93–1.84 (m, 2H), 1.81–1.72 (m, 1H), 1.68–1.45 (m, 8H), 1.19 (s, 6H). ^{13}C NMR (126 MHz, DMSO-d_6) δ 162.0, 159.9, 157.3, 156.9, 151.1, 150.7, 148.3, 139.6, 131.8, 126.2, 120.6, 114.9, 114.6, 113.6, 68.5, 68.3, 61.7, 43.7, 30.2, 29.3, 28.8, 28.0, 25.0, 24.6, 24.0, 20.3, 19.0. HRMS: calcd for $C_{29}H_{38}N_5O_3$ $[M + H]^+$, 504.2975; found, 504.2966.

***trans*-7-Fluoro-*N*-(4-(5-((4-hydroxy-4-methylpentyl)oxy)-2-methylphenyl)pyridin-2-yl)-5-phenyl-6,7-dihydro-5*H*-pyrrolo[1,2-*b*][1,2,4]triazole-2-carboxamide (13).** Purified by preparative thin layer chromatography (dichloromethane : methanol = 20 : 1, V : V) as a white solid, yield 42%. ^{1}H NMR (400 MHz, chloroform-d) δ 9.56 (s, 1H), 8.43–8.40 (m, 1H), 8.37 (d, J = 5.1 Hz, 1H), 7.47–7.41 (m, 3H), 7.23–7.17 (m, 3H), 7.08 (dd, J = 5.2, 1.5 Hz, 1H), 6.88 (dd, J = 8.3, 2.8 Hz, 1H), 6.84 (d, J = 2.7 Hz, 1H), 6.13 (dd, $^{2}J_{H-F}$ = 55.4 Hz, J = 6.2 Hz, 1H), 5.78 (td, J = 6.6, 3.1 Hz, 1H), 4.01 (t, J = 6.3 Hz, 2H), 3.52–3.38 (m, 1H), 3.17–3.01 (m, 2H), 2.83 (d, J = 0.6 Hz, 3H), 2.27 (s, 3H), 1.96–1.86 (m, 2H), 1.70–1.66 (m, 2H), 1.28 (s, 6H). ^{13}C NMR (126 MHz, DMSO-d_6) δ 161.7, 158.7 ($^{2}J_{C-F}$ = 22 Hz), 156.9, 151.1, 150.6, 148.3, 139.5, 137.3, 131.8, 128.9, 128.8, 127.3, 126.1, 120.8, 114.9, 114.6, 114.1, 83.4 ($^{1}J_{C-F}$ = 178.0 Hz), 68.5, 68.3, 60.4, 44.1 ($^{2}J_{C-F}$ = 23.0 Hz), 38.2, 29.3, 24.0, 19.0. HRMS: calcd for $C_{30}H_{33}FN_5O_3$ $[M + H]^+$, 530.2567; found, 530.2559.

***cis*-7-Fluoro-*N*-(4-(5-((4-hydroxy-4-methylpentyl)oxy)-2-methylphenyl)pyridin-2-yl)-5-phenyl-6,7-dihydro-5*H*-pyrrolo[1,2-*b*][1,2,4]triazole-2-carboxamide (14).** Purified by preparative thin layer chromatography (dichloromethane : methanol = 20 : 1, V : V) as a white solid, yield 38%. ^{1}H NMR (400 MHz, chloroform-d) δ 9.53 (s, 1H), 8.38 (s, 1H), 8.34 (d, J = 4.8 Hz, 1H), 7.39 (s, 3H), 7.17 (d, J = 8.1 Hz, 1H), 7.05 (d, J = 4.7 Hz, 1H), 6.85 (d, J = 8.1 Hz, 1H), 6.81 (s, 1H), 6.05 (dd, $^{2}J_{H-F}$ = 55.9 Hz, J = 7.0 Hz, 1H), 5.51 (s, 1H), 4.02–3.96 (m, 2H), 3.75–3.58 (m, 1H), 3.07–2.91 (m, 1H), 2.23 (s, 3H), 1.92–1.83 (m, 2H), 1.68–1.63 (m, 2H), 1.25 (s, 6H). ^{13}C NMR (126 MHz, DMSO-d_6) δ 161.8, 158.7 ($^{2}J_{C-F}$ = 23.0 Hz), 156.9, 151.1, 150.6, 148.3, 139.5, 138.3, 131.8, 129.0, 128.7, 126.7, 126.1, 120.8, 114.9, 114.6, 114.1, 83.2 ($^{1}J_{C-F}$ = 178.0 Hz), 68.5, 68.3, 60.1, 43.0 ($^{2}J_{C-F}$ = 22.0 Hz), 29.3, 24.0, 19.0. HRMS: calcd for $C_{30}H_{33}FN_5O_3$ $[M + H]^+$, 530.2567; found, 530.2564.

***N*-(5-Fluoro-4-(5-((4-hydroxy-4-methylpentyl)oxy)-2-methylphenyl)pyridin-2-yl)-5-phenyl-6,7-dihydro-5*H*-pyrrolo[1,2-*b*][1,2,4]triazole-2-carboxamide (15).** Purified by preparative thin layer chromatography(dichloromethane : methanol = 20 : 1, V : V) as a white solid, yield 55%.^{1}H NMR (400 MHz, acetone-d_6) δ 9.64 (s, 1H), 8.33 (d, J = 1.4 Hz, 1H),

8.30 (d, J = 5.6 Hz, 1H), 7.43–7.33 (m, 3H), 7.32–7.24 (m, 3H), 6.96 (dd, J = 8.4, 2.7 Hz, 1H), 6.88 (d, J = 2.7 Hz, 1H), 5.65 (dd, J = 8.3, 5.9 Hz, 1H), 4.01 (t, J = 6.6 Hz, 2H), 3.40–3.28 (m, 2H), 3.25–3.14 (m, 1H), 3.14–3.03 (m, 1H), 2.73 (s, 1H), 2.15 (s, 3H), 1.91–1.82 (m, 2H), 1.62–1.56 (m, 2H), 1.18 (s, 6H). ^{13}C NMR (126 MHz, DMSO-d_6) δ 162.7, 160.6, 157.1, 156.8, 153.1 ($^1J_{C-F}$ = 249.0 Hz), 147.1, 139.3, 138.1 ($^3J_{C-F}$ = 16.0 Hz), 136.2 ($^2J_{C-F}$ = 27.0 Hz), 133.6, 131.4, 128.9, 128.4, 127.1, 126.7, 115.6, 115.3, 115.1, 68.5, 68.4, 61.1, 35.4, 29.3, 23.9, 20.6, 18.4. HRMS: calcd for $C_{30}H_{33}FN_5O_3$ [M + H]$^+$, 530.2567; found, 530.2566.

***N*-(5-Chloro-4-(5-((4-hydroxy-4-methylpentyl)oxy)-2-methylphenyl)pyridin-2-yl)-5-phenyl-6,7-dihydro-5*H*-pyrrolo[1,2-*b*][1,2,4]triazole-2-carboxamide (16).** Purified by preparative thin layer chromatography (dichloromethane : methanol = 20 : 1, V : V) as a white solid, yield 52%. ^{1}H NMR (400 MHz, acetone-d_6) δ 9.64 (s, 1H), 8.44 (s, 1H), 8.27 (s, 1H), 7.44–7.34 (m, 3H), 7.30 (d, J = 7.3 Hz, 2H), 7.25 (d, J = 8.6 Hz, 1H), 6.95 (dd, J = 8.4, 2.6 Hz, 1H), 6.78 (s, 1H), 5.66 (t, J = 7.3 Hz, 1H), 4.01 (t, J = 6.6 Hz, 2H), 3.39 (s, 1H), 3.27–3.17 (m, 2H), 3.16–3.09 (m, 1H), 1.91–1.84 (m, 2H), 1.62–1.57 (m, 2H), 1.18 (s, 6H). ^{13}C NMR (126 MHz, DMSO-d_6) δ 162.7, 160.5, 157.3, 156.7, 149.5, 149.4, 147.5, 139.3, 137.2, 131.2, 128.9, 128.4, 126.8, 126.4, 125.3, 115.2, 115.0, 114.3, 68.5, 68.3, 61.1, 35.4, 29.3, 23.9, 20.6, 18.2. HRMS: calcd for $C_{30}H_{33}ClN_5O_3$ [M + H]$^+$, 546.2272; found, 546.2263.

***N*-(4-(5-((4-Hydroxy-4-methylpentyl)oxy)-2-methylphenyl)-5-methylpyridin-2-yl)-5-phenyl-6,7-dihydro-5*H*-pyrrolo[1,2-*b*][1,2,4]triazole-2-carboxamide (17).** Purified by preparative thin layer chromatography (dichloromethane : methanol = 20 : 1, V : V) as a white solid, yield 43%. ^{1}H NMR (400 MHz, acetone-d_6) δ 9.52 (s, 1H), 8.28 (s, 1H), 8.11 (s, 1H), 7.45–7.38 (m, 3H), 7.35–7.29 (m, 2H), 7.25 (d, J = 8.4 Hz, 1H), 6.92 (dd, J = 8.4, 2.8 Hz, 1H), 6.72 (d, J = 2.7 Hz, 1H), 5.67 (dd, J = 8.3, 5.9 Hz, 1H), 4.02 (t, J = 6.6 Hz, 2H), 3.44–3.34 (m, 1H), 3.27–3.18 (m, 2H), 3.18–3.08 (m, 1H), 2.81 (s, 3H), 2.75 (s, 1H), 2.02 (s, 3H), 1.91–1.85 (m, 2H), 1.64–1.59 (m, 2H), 1.20 (s, 6H). ^{13}C NMR (126 MHz, DMSO-d_6) δ 162.6, 160.7, 157.0, 156.7, 150.9, 148.9, 148.7, 139.3, 131.2, 128.9, 128.4, 127.4, 126.7, 125.9, 114.3, 113.9, 113.3, 68.5, 68.2, 61.0, 35.4, 29.3, 23.9, 20.6, 18.3, 15.8. HRMS: calcd for $C_{31}H_{36}N_5O_3$ [M + H]$^+$, 526.2818; found, 526.2813.

***N*-(5-(5-((4-Hydroxy-4-methylpentyl)oxy)-2-methylphenyl)pyridazin-3-yl)-5-phenyl-6,7-dihydro-5*H*-pyrrolo[1,2-*b*][1,2,4]triazole-2-carboxamide (18).** Purified by preparative thin layer chromatography (dichloromethane : methanol = 20 : 1, V : V) as a white solid, yield 28%. ^{1}H NMR (400 MHz, acetone-d_6) δ 10.13 (s, 1H), 9.70 (d, J = 2.5 Hz, 1H), 8.33 (d, J = 2.5 Hz, 1H), 7.46–7.35 (m, 3H), 7.32–7.23 (m, 3H), 7.06 (d, J = 2.6 Hz, 1H), 6.96 (d, J = 8.7 Hz, 1H), 5.66 (t, J = 7.1 Hz, 1H), 4.04 (t, J = 6.6 Hz, 2H), 3.43–3.31 (m, 1H), 3.30 (s, 1H), 3.26–3.17 (m, 1H), 3.16–3.06 (m, 1H), 2.31 (s, 3H), 1.92–1.85 (m, 2H), 1.64–1.58 (m, 2H), 1.19 (s, 6H). ^{13}C NMR (126 MHz, DMSO-d_6) δ 162.9, 161.0, 160.4, 158.8, 156.9, 142.4, 139.4, 138.2, 137.7, 131.9, 128.9, 128.4, 127.2, 126.8, 115.4, 115.3, 115.2, 68.5, 68.3, 61.1, 35.5, 29.3, 24.0, 20.5, 19.0. HRMS: calcd for $C_{29}H_{33}N_6O_3$ [M + H]$^+$, 513.2614; found, 513.2605.

***N*-(4-(2-Chloro-5-((4-hydroxy-4-methylpentyl)oxy)phenyl)pyridin-2-yl)-5-phenyl-6,7-dihydro-5*H*-pyrrolo[1,2-*b*][1,2,4]triazole-2-carboxamide (19).** Purified by preparative thin layer chromatography (dichloromethane : methanol = 20 : 1, V : V) as a white solid, yield 49%. ^{1}H NMR (400 MHz, acetone-d_6) δ 9.61 (s, 1H), 8.47–8.39 (m, 2H), 7.46 (d, J = 8.4 Hz, 1H), 7.43–7.36 (m, 3H), 7.33–7.30 (m, 2H), 7.25 (dd, J = 5.3, 1.4 Hz, 1H), 7.07–7.02 (m, 2H), 5.67 (dd, J = 8.3, 6.0 Hz, 1H), 4.08 (t, J = 6.6 Hz, 2H), 3.44–3.28 (m, 2H), 3.26 (s, 1H), 3.23–3.07 (m, 2H), 1.94–1.85 (m, 2H), 1.65–1.57 (m, 2H), 1.19 (s, 6H). ^{13}C NMR (126 MHz, DMSO-d_6) δ 162.7, 160.6, 157.8, 157.2, 150.7, 148.5, 148.4, 139.3, 138.2, 131.0, 128.9, 128.4, 126.8, 121.8, 120.8, 116.7, 116.5, 113.9, 68.8, 68.5, 61.1, 35.4, 29.3, 23.8, 20.6. HRMS: calcd for $C_{29}H_{31}ClN_5O_3$ [M + H]$^+$, 532.2115; found, 532.2109.

***N*-(4-(3-((4-Hydroxy-4-methylpentyl)oxy)phenyl)pyridin-2-yl)-5-phenyl-6,7-dihydro-5*H*-pyrrolo[1,2-*b*][1,2,4]triazole-2-carboxamide (20).** Purified by preparative thin layer chromatography (dichloromethane : methanol = 20 : 1, V : V) as a white solid, yield 58%. ^{1}H NMR (400 MHz, acetone-d_6) δ 9.59 (s, 1H), 8.64 (s, 1H), 8.41 (d, J = 5.3 Hz, 1H), 7.50–7.38 (m, 5H), 7.37–7.30 (m, 4H), 7.08 (d, J = 8.3 Hz, 1H), 5.69 (t, J = 7.3 Hz, 1H), 4.13 (t, J = 6.5 Hz, 2H), 3.45–3.33 (m, 1H), 3.29 (d, J = 1.5 Hz, 1H), 3.25–3.09 (m, 2H), 2.81–2.69 (m, 1H), 1.99–1.88 (m, 2H), 1.70–1.61 (m, 2H), 1.22 (s, 6H). ^{13}C NMR (126 MHz, DMSO-d_6) δ 162.7, 160.6, 159.3, 157.2, 151.3, 149.5, 148.9, 139.3, 138.8, 130.5, 128.9, 128.4, 126.8, 118.9, 118.2, 115.3, 112.9, 111.1, 68.5, 68.4, 61.1, 35.4, 29.3, 23.9, 20.6. HRMS: calcd for $C_{29}H_{32}N_5O_3$ [M + H]$^+$, 498.2505; found, 498.2502.

***N*-(4-(5-Methoxy-2-methylphenyl)pyridin-2-yl)-5-phenyl-6,7-dihydro-5*H*-pyrrolo[1,2-*b*][1,2,4]triazole-2-carboxamide (21).** Purified by preparative thin layer chromatography (dichloromethane : methanol = 20 : 1, V : V) as a white solid, yield 53%. ^{1}H NMR (400 MHz, acetone-d_6) δ 9.58 (s, 1H), 8.39 (d, J = 5.1 Hz, 1H), 8.32 (d, J = 1.4 Hz, 1H), 7.44–7.35 (m, 3H), 7.34–7.29 (m, 2H), 7.25 (d, J = 8.5 Hz, 1H), 7.15 (dd, J = 5.2, 1.5 Hz, 1H), 6.92 (dd, J = 8.5, 2.8 Hz, 1H), 6.85 (d, J = 2.8 Hz, 1H), 5.69–5.64 (m, 1H), 3.81 (s, 3H), 3.44–3.33 (m, 1H), 3.27–3.17 (m, 1H), 3.16–3.05 (m, 1H), 2.80 (s, 1H), 2.79–2.69 (m, 1H), 2.23 (s, 3H). ^{13}C NMR (126 MHz, DMSO-d_6) δ 162.7, 160.6, 157.5, 157.2, 151.1, 150.7, 148.3, 139.6, 139.3, 131.7, 128.9, 128.4, 126.8, 126.3, 120.7, 114.3, 114.1, 113.7, 61.1, 55.2, 35.4, 20.6, 19.0. HRMS: calcd for $C_{25}H_{24}N_5O_2$ [M + H]$^+$, 426.1930; found, 426.1925.

***N*-(4-(5-(2-Hydroxy-2-methylpropoxy)-2-methylphenyl)pyridin-2-yl)-5-phenyl-6,7-dihydro-5*H*-pyrrolo[1,2-*b*][1,2,4]triazole-2-carboxamide (22).** Purified by preparative thin layer chromatography (dichloromethane : methanol = 20 : 1, V : V) as a white solid, yield 45%. ^{1}H NMR (400 MHz, acetone-d_6) δ 9.58 (s, 1H), 8.39 (d, J = 5.1 Hz, 1H), 8.32 (s, 1H), 7.45–7.34 (m, 3H), 7.33–7.28 (m, 2H), 7.24 (d, J = 8.4 Hz, 1H), 7.16 (dd, J = 5.1, 1.6 Hz, 1H), 6.95 (dd, J = 8.5, 2.8 Hz, 1H), 6.88 (d, J = 2.6 Hz, 1H), 5.74–5.63 (m, 1H), 3.83 (s, 2H), 3.72 (s, 1H),

3.42–3.32 (m, 1H), 3.28–3.18 (m, 1H), 3.18–3.07 (m, 1H), 2.79–2.74 (m, 1H), 2.23 (s, 3H), 1.28 (s, 6H). ^{13}C NMR (126 MHz, DMSO-d_6) δ 162.7, 160.6, 157.2, 151.1, 150.7, 148.3, 139.5, 139.3, 131.8, 128.9, 128.4, 126.8, 126.5, 126.2, 120.6, 115.1, 114.8, 113.7, 76.3, 68.6, 61.1, 35.4, 26.6, 20.6, 19.0. HRMS: calcd for $C_{28}H_{30}N_5O_3$ $[M + H]^+$, 484.2349; found, 484.2347.

***N*-(4-(2-Methyl-5-(2-(tetrahydro-2*H*-pyran-4-yl)ethoxy) phenyl)pyridin-2-yl)-5-phenyl-6,7-dihydro-5*H*-pyrrolo[1,2-*b*] [1,2,4]triazole-2-carboxamide (23).** Purified by preparative thin layer chromatography (dichloromethane : methanol = 20 : 1, V : V) as a white solid, yield 38%. ^{1}H NMR (400 MHz, acetone-d_6) δ 9.58 (s, 1H), 8.39 (d, J = 5.1 Hz, 1H), 8.32 (s, 1H), 7.45–7.34 (m, 3H), 7.34–7.29 (m, 2H), 7.24 (d, J = 8.4 Hz, 1H), 7.15 (dd, J = 5.2, 1.5 Hz, 1H), 6.92 (dd, J = 8.3, 2.8 Hz, 1H), 6.86 (d, J = 2.7 Hz, 1H), 5.66 (dd, J = 8.3, 6.0 Hz, 1H), 4.08 (t, J = 6.4 Hz, 2H), 3.92–3.81 (m, 2H), 3.43–3.26 (m, 3H), 3.26–3.16 (m, 1H), 3.16–3.07 (m, 1H), 2.79–2.67 (m, 1H), 2.23 (s, 3H), 1.75–1.63 (m, 4H), 1.32–1.25 (m, 3H). ^{13}C NMR (126 MHz, DMSO-d_6) δ 162.7, 160.6, 157.2, 156.8, 151.1, 150.7, 148.3, 139.5, 139.3, 131.7, 128.9, 128.4, 126.8, 126.2, 120.7, 114.9, 114.7, 113.7, 67.0, 65.1, 61.1, 35.6, 35.4, 32.6, 31.5, 20.6, 19.0. HRMS: calcd for $C_{31}H_{34}N_5O_3$ $[M + H]^+$, 524.2662; found, 524.2660.

***N*-(4-(5-(3-Cyanopropoxy)-2-methylphenyl)pyridin-2-yl)-5-phenyl-6,7-dihydro-5*H*-pyrrolo[1,2-*b*][1,2,4]triazole-2-carboxamide (24).** Purified by preparative thin layer chromatography (dichloromethane : methanol = 20 : 1, V : V) as a white solid, yield 53%. ^{1}H NMR (400 MHz, methanol-d_4) δ 8.35 (d, J = 5.2 Hz, 1H), 8.25 (s, 1H), 7.43–7.33 (m, 3H), 7.29–7.20 (m, 3H), 7.18–7.12 (m, 1H), 6.93 (dd, J = 8.3, 2.7 Hz, 1H), 6.84 (d, J = 2.7 Hz, 1H), 5.60 (t, J = 7.2 Hz, 1H), 4.08 (t, J = 5.9 Hz, 2H), 3.27 (s, 1H), 3.18 (dd, J = 9.4, 4.4 Hz, 1H), 3.14–3.05 (m, 1H), 2.76–2.67 (m, 1H), 2.64 (t, J = 7.1 Hz, 2H), 2.22 (s, 3H), 2.16–2.05 (m, 2H). ^{13}C NMR (126 MHz, DMSO-d_6) δ 162.7, 160.6, 157.2, 156.5, 151.0, 150.7, 148.3, 139.6, 139.3, 131.8, 128.9, 128.4, 126.8, 120.6, 120.3, 115.0, 114.7, 113.7, 65.9, 61.1, 35.4, 24.7, 20.6, 19.0, 13.3. HRMS: calcd for $C_{28}H_{27}N_6O_2$ $[M + H]^+$, 479.2195; found, 479.2193.

***(R,R)*-7-Fluoro-*N*-(4-(2-methyl-5-(2-morpholinoethoxy) phenyl)pyridin-2-yl)-5-phenyl-6,7-dihydro-5*H*-pyrrolo[1,2-*b*] [1,2,4]triazole-2-carboxamide (25).** Purified by preparative thin layer chromatography (dichloromethane : methanol = 15 : 1, V : V) as a white solid, yield 40%. ^{1}H NMR (600 MHz, methanol-d_4) δ 8.37 (d, J = 5.2 Hz, 1H), 8.25 (s, 1H), 7.46–7.37 (m, 3H), 7.33–7.29 (m, 2H), 7.23 (d, J = 8.4 Hz, 1H), 7.19–7.15 (m, 1H), 6.95–6.91 (m, 1H), 6.85 (d, J = 2.7 Hz, 1H), 6.15 (dd, $^2J_{H-F}$ = 56.3 Hz, J = 7.1 Hz, 1H), 5.70–5.64 (m, 1H), 4.15 (t, J = 5.5 Hz, 2H), 3.84–3.74 (m, 1H), 3.71 (t, J = 4.7 Hz, 4H), 2.90–2.83 (m, 1H), 2.81 (t, J = 5.4 Hz, 2H), 2.60 (t, J = 4.7 Hz, 4H), 2.23 (s, 3H). ^{13}C NMR (126 MHz, DMSO-d_6) δ 161.8, 158.7 ($^2J_{C-F}$ = 22.0 Hz), 156.9, 156.7, 151.0, 150.6, 148.3, 139.5, 138.3, 131.8, 129.0, 128.7, 126.7, 126.4, 120.8, 114.9, 114.8, 114.1, 83.2 ($^1J_{C-F}$ = 178.0 Hz), 66.2, 65.5, 60.1, 57.0, 53.6, 43.0 ($^2J_{C-F}$ = 22.0 Hz), 19.0. HRMS: calcd for $C_{30}H_{32}FN_6O_3$ $[M + H]^+$, 543.2520; found, 543.2518.

***(S,S)*-7-Fluoro-*N*-(4-(2-methyl-5-(2-morpholinoethoxy) phenyl)pyridin-2-yl)-5-phenyl-6,7-dihydro-5*H*-pyrrolo[1,2-*b*] [1,2,4]triazole-2-carboxamide (26).** Purified by preparative thin layer chromatography (dichloromethane : methanol = 15 : 1, V : V) as a white solid, yield 43%. ^{1}H NMR (600 MHz, methanol-d_4) δ 8.37 (d, J = 5.2 Hz, 1H), 8.25 (s, 1H), 7.46–7.37 (m, 3H), 7.33–7.29 (m, 2H), 7.23 (d, J = 8.4 Hz, 1H), 7.19–7.15 (m, 1H), 6.95–6.91 (m, 1H), 6.85 (d, J = 2.7 Hz, 1H), 6.15 (dd, $^2J_{H-F}$ = 56.3 Hz, J = 7.1 Hz, 1H), 5.70–5.64 (m, 1H), 4.15 (t, J = 5.5 Hz, 2H), 3.84–3.74 (m, 1H), 3.71 (t, J = 4.7 Hz, 4H), 2.90–2.83 (m, 1H), 2.81 (t, J = 5.4 Hz, 2H), 2.60 (t, J = 4.7 Hz, 4H), 2.23 (s, 3H). ^{13}C NMR (126 MHz, DMSO-d_6) δ 161.8, 158.7 ($^2J_{C-F}$ = 22.0 Hz), 156.9, 156.7, 151.0, 150.6, 148.3, 139.5, 138.3, 131.8, 129.0, 128.7, 126.7, 126.4, 120.8, 114.9, 114.8, 114.1, 83.2 ($^1J_{C-F}$ = 178.0 Hz), 66.2, 65.5, 60.1, 57.0, 53.6, 43.0 ($^2J_{C-F}$ = 22.0 Hz), 19.0. HRMS: calcd for $C_{30}H_{32}FN_6O_3$ $[M + H]^+$, 543.2520; found, 543.2515.

***(R,R)*-7-Fluoro-*N*-(4-(2-methyl-5-(2-(tetrahydro-2*H*-pyran-4-yl)ethoxy)phenyl)pyridin-2-yl)-5-phenyl-6,7-dihydro-5*H*-pyrrolo[1,2-*b*][1,2,4]triazole-2-carboxamide (27).** Purified by preparative thin layer chromatography (dichloromethane : methanol = 15 : 1, V : V) as a white solid, yield 40%. ^{1}H NMR (600 MHz, methanol-d_4) δ 8.38 (d, J = 5.1 Hz, 1H), 8.26 (s, 1H), 7.46–7.39 (m, 3H), 7.33 (d, J = 7.4 Hz, 2H), 7.23 (d, J = 8.5 Hz, 1H), 7.18 (d, J = 5.0 Hz, 1H), 6.91 (d, J = 8.5 Hz, 1H), 6.82 (s, 1H), 6.16 (dd, $^2J_{H-F}$ = 56.2 Hz, J = 7.1 Hz, 1H), 5.69 (d, J = 8.3 Hz, 1H), 4.06 (t, J = 6.4 Hz, 2H), 3.97–3.90 (m, 2H), 3.86–3.75 (m, 1H), 3.43 (t, J = 11.8 Hz, 2H), 2.87 (dd, J = 26.6, 15.2 Hz, 1H), 2.24 (s, 3H), 1.83 (s, 1H), 1.76–1.68 (m, 4H), 1.40–1.28 (m, 2H). ^{13}C NMR (126 MHz, DMSO-d_6) δ 161.8, 158.7 ($^2J_{C-F}$ = 22.0 Hz), 156.9, 156.9, 151.1, 150.6, 148.3, 139.5, 138.2, 131.8, 129.0, 128.7, 126.7, 126.2, 120.8, 114.9, 114.7, 114.1, 83.2 ($^1J_{C-F}$ = 178.0 Hz), 67.0, 65.1, 60.1, 43.0 ($^2J_{C-F}$ = 22.0 Hz), 35.6, 32.6, 31.5, 19.0. HRMS: calcd for $C_{31}H_{33}FN_5O_3$ $[M + H]^+$, 542.2567; found, 542.2560.

***(S,S)*-7-Fluoro-*N*-(4-(2-methyl-5-(2-(tetrahydro-2*H*-pyran-4-yl) ethoxy)phenyl)pyridin-2-yl)-5-phenyl-6,7-dihydro-5*H*-pyrrolo[1,2-*b*][1,2,4]triazole-2-carboxamide (28).** Purified by preparative thin layer chromatography (dichloromethane : methanol = 15 : 1, V : V) as a white solid, yield 39%. ^{1}H NMR (600 MHz, methanol-d_4) δ 8.38 (d, J = 5.1 Hz, 1H), 8.26 (s, 1H), 7.46–7.39 (m, 3H), 7.33 (d, J = 7.4 Hz, 2H), 7.23 (d, J = 8.5 Hz, 1H), 7.18 (d, J = 5.0 Hz, 1H), 6.91 (d, J = 8.5 Hz, 1H), 6.82 (s, 1H), 6.16 (dd, $^2J_{H-F}$ = 56.2 Hz, J = 7.1 Hz, 1H), 5.69 (d, J = 8.3 Hz, 1H), 4.06 (t, J = 6.4 Hz, 2H), 3.97–3.90 (m, 2H), 3.86–3.75 (m, 1H), 3.43 (t, J = 11.8 Hz, 2H), 2.87 (dd, J = 26.6, 15.2 Hz, 1H), 2.24 (s, 3H), 1.83 (s, 1H), 1.76–1.68 (m, 4H), 1.40–1.28 (m, 2H). ^{13}C NMR (126 MHz, DMSO-d_6) δ 161.8, 158.7 ($^2J_{C-F}$ = 22.0 Hz), 156.9, 156.9, 151.1, 150.6, 148.3, 139.5, 138.2, 131.8, 129.0, 128.7, 126.7, 126.2, 120.8, 114.9, 114.7, 114.1, 83.2 ($^1J_{C-F}$ = 178.0 Hz), 67.0, 65.1, 60.1, 43.0 ($^2J_{C-F}$ = 22.0 Hz), 35.6, 32.6, 31.5, 19.0. HRMS: calcd for $C_{31}H_{33}FN_5O_3$ $[M + H]^+$, 542.2567; found, 542.2565.

Biology

Kinase inhibition assay. The RIPK1 inhibitory activities of compounds were evaluated using the ADP-Glo Assay Kit

(Promega, United States) according to the instructions. Then, a SpectraMax Paradigm reader (MD) was used to record the luminescence. Inhibition% = ((specific signal (DMSO control) − specific signal (inhibitor))/(specific signal (DMSO control))) × 100%.

Necroptosis induction and cell viability assays. I2.1 and Hepa1-6 cells were purchased from American Type Culture Collection (ATCC, Manassas, VA, USA). I2.1 and Hepa1-6 cells were seeded in 96-well plates with growth media at a low density, and incubated overnight. For I2.1 cells, designated concentrations of the tested compounds were added to each well. After 1 h, the cells were stimulated with 20 ng mL^{-1} TNF-α and the cells were further incubated for 24 h. For Hepa1-6 cells, on the following day, cells were treated with TNF-α (20 ng mL^{-1}) and BV6 (10 μM) to induce necroptosis, and treated with different concentrations of the tested compounds for 24 h. Z-VAD (10 μM) was added 1 h prior to the addition of the above treatments. Finally, the effect of the tested compounds against I2.1 and Hepa1-6 cell viability was determined using a cell counting kit (CCK-8) (Dojindo, Japan) assay.

Pharmacokinetic evaluation. Compound **26** was dissolved in DMSO/0.5% HMPC (5/95, v/v) and administered orally to Sprague Dawley (SD) rats (male, $N = 3$). Blood samples were collected at 0.25, 0.5, 1, 2, 4, 8, and 24 h after p.o. administration, and the concentrations of compound **26** in serum were determined by LC-MS/MS.

All animal procedures were performed in accordance with the Guidelines for Care and Use of Laboratory Animals of Shanghai Institute of Materia Medica and approved by the Animal Ethics Committee of Shanghai Institute of Materia Medica (approval no. 2023-01-YY-26).

Molecular docking study. The docking studies were carried out with Maestro 11.0 using the crystal structure (PDB code: 6NYH) obtained from the RCSB Protein Data Bank as the receptor. Both bond orders and hydrogen atoms were optimized, and water molecules were removed. The docking box was set to 14 Å × 14 Å × 14 Å and centered at the native ligand. Compound **26** was prepared with LigPrep with the OPLS force field. Then compound **26** was docked into the well-defined docking grids with the standard precision (SP) mode. Fig. 3 was generated with PyMOL version 1.3.

Author contributions

Z. J. and Y. D. contributed equally to this article. Z. J. and Y. D.: investigation, methodology, writing – original draft. Y. J. and X. P.: investigation, methodology. W. D.: conceptualization, supervision, writing – review & editing. H. Z. and J. A.: conceptualization, investigation, supervision, writing – review & editing.

Conflicts of interest

The authors declare that they have no known competing financial interests.

Acknowledgements

This work was supported by China Postdoctoral Science Foundation (Certificate Number: 2023T160663), Institutes for Drug Discovery and Development, Chinese Academy of Sciences (No. SIMM0320231002), the Natural Science Foundation of China for Innovation Research Group (No. 81821005), the Project of Shanghai Institute of Materia Medica, Chinese Academy of Sciences (No. SIMM0120231001) and the Shandong Laboratory Program (SYS202205).

References

1 K. Yamanaka, Y. Saito, T. Yamamori, Y. Urano and N. Noguchi, *J. Biol. Chem.*, 2011, **286**, 24666–24673.
2 R. L. Ang, M. Chan and A. T. Ting, *Front. Cell Dev. Biol.*, 2019, **7**, 163.
3 W. Wu, X. Wang, N. Berleth, J. Deitersen, N. Wallot-Hieke, P. Böhler, D. Schlütermann, F. Stuhldreier, J. Cox, K. Schmitz, S. Seggewiß, C. Peter, G. Kasof, A. Stefanski, K. Stühler, A. Tschapek, A. Gödecke and B. Stork, *Cell Rep.*, 2020, **31**, 107547.
4 N. Festjens, T. Vanden Berghe, S. Cornelis and P. Vandenabeele, *Cell Death Differ.*, 2007, **14**, 400–410.
5 D. Bertheloot, E. Latz and B. S. Franklin, *Cell. Mol. Immunol.*, 2021, **18**, 1106–1121.
6 C. Xu, J. Wu, Y. Wu, Z. Ren, Y. Yao, G. Chen, E. F. Fang, J. H. Noh, Y. U. Liu, L. Wei, X. Chen and J. Sima, *Theranostics*, 2021, **11**, 9452–9469.
7 L. Jin, P. Liu, M. Yin, M. Zhang, Y. Kuang and W. Zhu, *J. Dermatol. Sci.*, 2020, **99**, 146–151.
8 A. Q. Chen, Z. Fang, X. L. Chen, S. Yang, Y. F. Zhou, L. Mao, Y. P. Xia, H. J. Jin, Y. N. Li, M. F. You, X. X. Wang, H. Lei, Q. W. He and B. Hu, *Cell Death Dis.*, 2019, **10**, 487.
9 L. He, K. Peng, Y. Liu, J. Xiong and F. F. Zhu, *Onco Targets Ther*, 2013, **6**, 1539–1543.
10 S. Park, K. J. Hatanpaa, Y. Xie, B. E. Mickey, C. J. Madden, J. M. Raisanen, D. B. Ramnarain, G. Xiao, D. Saha, D. A. Boothman, D. Zhao, R. M. Bachoo, R. O. Pieper and A. A. Habib, *Cancer Res.*, 2009, **69**, 2809–2816.
11 Q. Wang, W. Chen, X. Xu, B. Li, W. He, M. T. Padilla, J. H. Jang, T. Nyunoya, S. Amin, X. Wang and Y. Lin, *Carcinogenesis*, 2013, **34**, 2119–2128.
12 L. Seifert, G. Werba, S. Tiwari, N. N. Giao Ly, S. Alothman, D. Alqunaibit, A. Avanzi, R. Barilla, D. Daley, S. H. Greco, A. Torres-Hernandez, M. Pergamo, A. Ochi, C. P. Zambirinis, M. Pansari, M. Rendon, D. Tippens, M. Hundeyin, V. R. Mani, C. Hajdu, D. Engle and G. Miller, *Nature*, 2016, **532**, 245–249.
13 S. Hofmans, L. Devisscher, S. Martens, D. Van Rompaey, K. Goossens, T. Divert, W. Nerinckx, N. Takahashi, H. De Winter, P. Van Der Veken, V. Goossens, P. Vandenabeele and K. Augustyns, *J. Med. Chem.*, 2018, **61**, 1895–1920.
14 A. Fauster, M. Rebsamen, K. V. Huber, J. W. Bigenzahn, A. Stukalov, C. H. Lardeau, S. Scorzoni, M. Bruckner, M. Gridling, K. Parapatics, J. Colinge, K. L. Bennett, S. Kubicek,

S. Krautwald, A. Linkermann and G. Superti-Furga, *Cell Death Dis.*, 2015, **6**, e1767.
15 Halia Therapeutics Inc., *WO Pat.*, 2022212326A1, 2022.
16 Y. Qin, D. Li, C. Qi, H. Xiang, H. Meng, J. Liu, S. Zhou, X. Gong, Y. Li, G. Xu, R. Zu, H. Xie, Y. Xu, G. Xu, Z. Zhang, S. Chen, L. Pan, Y. Li and L. Tan, *Acta Pharm. Sin. B*, 2024, **14**, 319–334.
17 J. J. Fang, H. Z. Yao, C. Zhuang and F. E. Chen, *J. Med. Chem.*, 2023, **66**, 15288–15308.
18 Y. Sun, L. Xu, H. Shao, D. Quan, Z. Mo, J. Wang, W. Zhang, J. Yu, C. Zhuang and K. Xu, *J. Med. Chem.*, 2022, **65**, 14957–14969.
19 H. Zhang, L. Xu, X. Qin, X. Chen, H. Cong, L. Hu, L. Chen, Z. Miao, W. Zhang, Z. Cai and C. Zhuang, *J. Med. Chem.*, 2019, **62**, 6665–6681.
20 A. Degterev, Z. Huang, M. Boyce, Y. Li, P. Jagtap, N. Mizushima, G. D. Cuny, T. J. Mitchison, M. A. Moskowitz and J. Yuan, *Nat. Chem. Biol.*, 2005, **1**, 112–119.
21 P. A. Harris, S. B. Berger, J. U. Jeong, R. Nagilla, D. Bandyopadhyay, N. Campobasso, C. A. Capriotti, J. A. Cox, L. Dare, X. Dong, P. M. Eidam, J. N. Finger, S. J. Hoffman, J. Kang, V. Kasparcova, B. W. King, R. Lehr, Y. Lan, L. K. Leister, J. D. Lich, T. T. MacDonald, N. A. Miller, M. T. Ouellette, C. S. Pao, A. Rahman, M. A. Reilly, A. R. Rendina, E. J. Rivera, M. C. Schaeffer, C. A. Sehon, R. R. Singhaus, H. H. Sun, B. A. Swift, R. D. Totoritis, A. Vossenkämper, P. Ward, D. D. Wisnoski, D. Zhang, R. W. Marquis, P. J. Gough and J. Bertin, *J. Med. Chem.*, 2017, **60**, 1247–1261.
22 D. Tompson, M. Whitaker, R. Pan, G. Johnson, T. Fuller, V. Zann, L. McKenzie, K. Abbott-Banner, S. Hawkins and M. Powell, *Pharm. Res.*, 2022, **39**, 153–165.
23 P. A. Harris, J. M. Marinis, J. D. Lich, S. B. Berger, A. Chirala, J. A. Cox, P. M. Eidam, J. N. Finger, P. J. Gough, J. U. Jeong, J. Kang, V. Kasparcova, L. K. Leister, M. K. Mahajan, G. Miller, R. Nagilla, M. T. Ouellette, M. A. Reilly, A. R. Rendina, E. J. Rivera, H. H. Sun, J. H. Thorpe, R. D. Totoritis, W. Wang, D. Wu, D. Zhang, J. Bertin and R. W. Marquis, *ACS Med. Chem. Lett.*, 2019, **10**, 857–862.
24 GlaxoSmithKline, Study of GSK3845097 in previously treated participants with advanced synovial sarcoma and myxoid/round cell liposarcoma, **https://www.clinicaltrials.gov/study/NCT05943990**.
25 X. Yang, H. Lu, H. Xie, B. Zhang, T. Nie, C. Fan, T. Yang, Y. Xu, H. Su, W. Tang and B. Zhou, *Angew. Chem., Int. Ed.*, 2022, **61**, e202114922.
26 P. A. Harris, B. W. King, D. Bandyopadhyay, S. B. Berger, N. Campobasso, C. A. Capriotti, J. A. Cox, L. Dare, X. Dong, J. N. Finger, L. C. Grady, S. J. Hoffman, J. U. Jeong, J. Kang, V. Kasparcova, A. S. Lakdawala, R. Lehr, D. E. McNulty, R. Nagilla, M. T. Ouellette, C. S. Pao, A. R. Rendina, M. C. Schaeffer, J. D. Summerfield, B. A. Swift, R. D. Totoritis, P. Ward, A. Zhang, D. Zhang, R. W. Marquis, J. Bertin and P. J. Gough, *J. Med. Chem.*, 2016, **59**, 2163–2178.
27 M. Yoshikawa, M. Saitoh, T. Katoh, T. Seki, S. V. Bigi, Y. Shimizu, T. Ishii, T. Okai, M. Kuno, H. Hattori, E. Watanabe, K. S. Saikatendu, H. Zou, M. Nakakariya, T. Tatamiya, Y. Nakada and T. Yogo, *J. Med. Chem.*, 2018, **61**, 2384–2409.
28 P. A. Harris, N. Faucher, N. George, P. M. Eidam, B. W. King, G. V. White, N. A. Anderson, D. Bandyopadhyay, A. M. Beal, V. Beneton, S. B. Berger, N. Campobasso, S. Campos, C. A. Capriotti, J. A. Cox, A. Daugan, F. Donche, M. H. Fouchet, J. N. Finger, B. Geddes, P. J. Gough, P. Grondin, B. L. Hoffman, S. J. Hoffman, S. E. Hutchinson, J. U. Jeong, E. Jigorel, P. Lamoureux, L. K. Leister, J. D. Lich, M. K. Mahajan, J. Meslamani, J. E. Mosley, R. Nagilla, P. M. Nassau, S. L. Ng, M. T. Ouellette, K. K. Pasikanti, F. Potvain, M. A. Reilly, E. J. Rivera, S. Sautet, M. C. Schaeffer, C. A. Sehon, H. Sun, J. H. Thorpe, R. D. Totoritis, P. Ward, N. Wellaway, D. D. Wisnoski, J. M. Woolven, J. Bertin and R. W. Marquis, *J. Med. Chem.*, 2019, **62**, 5096–5110.
29 Beijing Scitech-MQ Pharmaceuticals Ltd., *WO Pat.*, 2020151589A1, 2020.
30 Genentech Inc., *CN Pat.*, 110023313A, 2019.
31 Hoffmann-La Roche, Genentech Inc., *WO Pat.*, 2019012063A1, 2019.
32 Genentech Inc., Hoffmann-La Roche, *WO Pat.*, 2022212809A1, 2022.